(29) Chung, T. C.; Kaufman, J. H.; Heeger, A. J.; Wudl, F. *Phys. Rev. B: Condens. Matter* **1984**, *30*, 702.
(30) Black, D. A.; Marynick, D. S.; Poropatic, P. A.; Reynolds, J. R., unpublished results.
(31) Martinez, M.; Reynolds, J. R.; Basak, S.; Black, D. A.; Marynick, D. S.; Pomerantz, M. *J. Polym. Sci., Polym. Phys. Ed.* **1988**, *26*, 911.
(32) Hartough, H. D., Ed. *The Chemistry of Heterocyclic Compounds: Thiophene and its Derivatives*; Interscience: New York, 1952.
(33) Brêdas, J. L.; Street, G. B. *Acc. Chem. Res.* **1985**, *18*, 309. Brêdas, J. L.; Tehemans, B.; Inipiat, J. G.; Andre, J. M.; Chance, R. R. *Phys. Rev. B: Condens. Matter* **1984**, *29*, 6761. Brêdas, J. L.; Scott, J. C.; Yakushi, K.; Street, G. B. *Phys. Rev. B: Condens. Matter* **1984**, *30*, 1023.
(34) Hotta, S.; Rughooputh, S. D. D. V.; Heeger, A. J. *Synth. Met.* **1987**, *22*, 79.
(35) Riga, J.; Snauwaert, P. H.; DePryck, A.; Lazzaroni, R.; Boutique, J. P.; Verbist, J. J.; Bredas, J. L.; Andre, J. M.; Taliani, C. *Synth. Met.* **1987**, *21*, 223. Themans, B.; Andre, J. M.; Bredas, J. L. *Synth. Met.* **1987**, *21*, 149.
(36) Tsai, E. W.; Basak, S.; Ruiz, J. P.; Reynolds, J. R.; Rajeshwar, K. *J. Electroanal. Chem.*, submitted for publication.
(37) Thakur, M. *Macromolecules* **1988**, *21*, 661.
(38) Roncali, J.; Yassar, A.; Garnier, F. *J. Chem. Soc., Chem. Commun.* **1988**, 581.
(39) Reynolds, J. R.; Hsu, S. G.; Arnott, H. J. *J. Polym. Sci., Polym. Phys. Ed.*, submitted for publication.
(40) Ofer, D.; Wrighton, M. S. *J. Am. Chem. Soc.* **1988**, *110*, 4467.
(41) Krische, B.; Zagorska, M. *Synth. Met.*, in press.

Theory of Block Copolymer Solutions: Nonselective Good Solvents

Glenn H. Fredrickson*

AT&T Bell Laboratories, Murray Hill, New Jersey 07974

Ludwik Leibler

Laboratoire de Physico-Chimie Theorique, E.S.P.C.I., 75231 Paris Cedex 05, France.
Received June 9, 1988; Revised Manuscript Received August 16, 1988

ABSTRACT: A theory to describe microphase separation and radiation scattering of AB diblock copolymers dissolved in a good, nonselective solvent is presented. In spite of the neutrality of the solvent, we find that the ordered microphases are inhomogeneous in solvent concentration as well as in copolymer composition. This arises from the ability of excess solvent at the interfaces between microdomains to screen unfavorable A–B interactions. It is also demonstrated that, unlike the melt, the microphase separation transition (MST) in copolymer solutions corresponds to a very narrow region of coexistence between a solvent-rich disordered phase and a solvent-poor ordered phase. The important semidilute regime is treated in detail—our analysis incorporates excluded volume swelling, corrections to scaling, and nonclassical fluctuation effects. For large molecular weights, the volume fraction of copolymer at the MST is predicted to scale as $\phi_t \sim N^{-0.62}$. Our results are consistent with previous measurements on copolymers in neutral solvents and suggest new experiments.

I. Introduction

Block copolymers have fascinated polymer scientists for many years, primarily because of the diversity of morphologies they exhibit.[1,2] In addition to the lamellar, cylindrical, and spherical microphases that have been known for some time, recent experiments on multiarm copolymers have turned up a new "ordered bicontinuous double-diamond" morphology,[3] a cocontinuous minimal surface structure that had previously been encountered only in multicomponent fluids containing surfactants. The variety of ordered structures that block copolymers possess and the unique control that the synthetic chemist has in determining those structures renders block copolymers very useful in commercial applications. For example, copolymers are used in high-impact-resistant plastics, membranes, photoresists, and adhesives and as compatibilizing additives to blends.

There has been much progress in the past decade with regard to our ability to predict the conditions (i.e., temperature, molecular weight, and composition) under which a molten block copolymer will exist in a particular morphological state. Building on the pioneering work of Williams and Leary[4] and Meier,[5] Helfand[6,7] developed an elegant statistical mechanical theory that allows comparison of the free energies of the various ordered phases and subsequent determination of the phase diagram. Helfand's theory is believed to be most accurate in the limit of strong incompatibility between the components of the copolymer, which is achieved by appropriate choice of monomers and at low temperature or high molecular weight. The theory also simplifies in this "strong segregation limit", where the interfacial thickness between microdomains is small relative to the characteristic size of a domain and one can employ the so-called narrow interface approximation.[6,7] Some interesting alternative approaches for treating the strong segregation limit have recently been published by Semenov[8] and by Ohta and Kawasaki.[9] One key prediction common to all the strong segregation theories is that the characteristic period of the ordered microphases scales as $N^{2/3}$, where N is the number of statistical segments per copolymer molecule. This prediction arises from a competition between the interfacial free energy and the entropy penalty associated with the non-Gaussian configurations chains must adopt to avoid passing through an interface.

Another important regime in molten block copolymers corresponds to the "weak segregation limit", which encompasses the compositionally disordered phase and the various ordered phases at temperatures very near the *microphase separation transition* (MST).[10] The MST is an order–disorder transition (similar to the crystallization of a one-component liquid) at which a disordered block copolymer melt first develops spatially periodic compositional order on lowering the temperature. In the weak segregation limit the ordered phases are not well-developed in the sense that the amplitudes of the compositional variations are very small and the boundaries between microdomains are not sharply defined. It is also believed

0024-9297/89/2222-1238$01.50/0

that the individual copolymer chains are only slightly perturbed from their ideal Gaussian distribution in this regime. The weak segregation limit is practically attained by employing block copolymer systems with compatible blocks and by working at high temperature and low molecular weight. A type of Landau theory for the weak segregation limit of diblock copolymer melts was developed by Leibler.[10] The theory provides an expression for the disordered phase scattering function that is in good agreement with neutron and X-ray experiments.[11,12] It also makes predictions for the location of the MST and for the coexistence of ordered phases very near the transition.

The Landau (mean field) theory[10] suggests that there are only two relevant parameters that govern the phase behavior of diblock copolymer melts in the weak segregation limit. The first parameter is f, the volume fraction of component A in the copolymer. Perfectly symmetric diblock molecules are characterized by $f = {}^1/_2$, whereas $f = 1$ and $f = 0$ correspond to the limits of pure homopolymer A or B, respectively. The second parameter in the Landau theory is the combination variable χN, the product of the Flory interaction parameter between A and B segments, χ, with the total number of statistical segments (monomers) per molecule, N. Polydispersity is not addressed by the theory. The mean-field approach of ref 10 leads to the prediction that the MST for symmetric diblock molecules is a *second*-order thermodynamic phase transition and occurs at $(\chi N)_c = 10.495$, while the MST for asymmetric diblocks ($f \neq {}^1/_2$) is *first* order and occurs at values of χN larger than 10.495. The lamellar morphology is predicted to appear at the MST for the perfectly symmetric case and a structure with a body-centered cubic (BCC) morphology (i.e., lattice of spheres) is expected at the MST for all other compositions. The theory also predicts that slightly asymmetric diblock melts can undergo further transitions from BCC to hexagonal arrays of cylinders (HEX) and then to lamellae (LAM) by increasing χN, e.g., by lowering temperature or increasing molecular weight. The complete melt phase diagram is shown in Figure 1 as a special case ($\phi = 1$) of the more general problem of a copolymer solution with volume fraction of polymer, ϕ.

The Landau theory, being mean field in nature, neglects the effects of order parameter fluctuations that become large in amplitude and coherent over large distances near the critical point at[10] $(\chi N)_c = 10.495$, $f_c = {}^1/_2$. Recently, Fredrickson and Helfand (FRH)[13] modified Leibler's approach for the weak segregation regime of molten diblock copolymers to take account of such fluctuations. On the basis of a self-consistent Hartree approximation, similar to that employed by Brazovskii[14] in his study of cholesteric liquid crystals, FRH showed that proper treatment of composition fluctuations leads (for finite molecular weight, symmetric copolymers) to a fluctuation-induced *first*-order phase transition[15] in place of the second-order transition predicted by mean-field theory. For the symmetric case the first-order transition was predicted[13] to occur at a lower temperature than the mean-field critical point: $(\chi N)_t = 10.495 + 41.022\,\bar{N}^{-1/3}$, where[32] $\bar{N} = Nb^6\rho_m{}^2 = (6R_g{}^2\rho_c{}^{2/3})^3$, with b the statistical segment length, ρ_m the number density of monomers, $\rho_c = \rho_m/N$ the number density of chains, and $R_g{}^2 = Nb^2/6$ the mean-squared radius of gyration. Hence, in the FRH theory there is an additional independent parameter, $\bar{N}$, proportional to the molecular weight, that is required to specify the phase diagram. Another important qualitative change from ref 10 is that the fluctuation corrections were found to open "windows" connecting the disordered (DIS) and LAM phases and

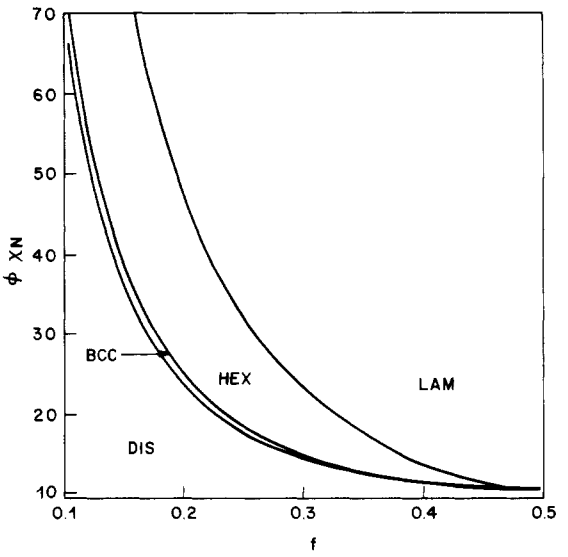

Figure 1. Mean-field phase diagram for diblock copolymer in a concentrated solution with a good, nonselective solvent. On the abscissa is the composition f, the fraction of statistical segments on each diblock that are of chemical species A. The ordinate is the combination variable $\phi\chi N$, the product of the polymer volume fraction, the Flory interaction parameter, and the number of statistical segments per copolymer molecule. In the limit $\phi \to 1$, Figure 1 reduces to the phase diagram obtained by Leibler.[10]

connecting the DIS and HEX phases. More precisely, direct first-order transitions were predicted between DIS and LAM for diblock copolymers with compositions in a band about $f = {}^1/_2$ (see Figure 3). Thus, in the FRH theory asymmetric melts can form structures other than BCC at the MST. As the molecular weight of the copolymers is increased and composition fluctuations are thereby suppressed, the widths of the DIS–LAM and DIS–HEX windows become smaller. Indeed, the FRH theory reduces exactly to Leibler's theory in the limit of infinite molecular weight.

On the experimental side, it has proven challenging to test these various theoretical predictions, particularly those appropriate for the weak segregation limit. One problem is that most commercially available copolymers contain blocks that are highly incompatible (i.e. have large χ) and as a consequence they are in the strong segregation limit even for quite low molecular weights. The disordered phase in such systems can rarely be accessed by increasing temperature, because thermal decomposition usually intervenes. A solution to this problem is to decrease molecular weight, but if this requires going to a very low degree of polymerization, many of the desirable polymeric properties may be lost. Another solution is to reformulate the block copolymer with very compatible blocks so that the disordered phase can be achieved at moderate molecular weight. This approach has been used very successfully by Bates[11,16] in his studies of the MST with isomeric blocks of 1,2-polybutadiene and 1,4-polybutadiene. Unfortunately, such materials are not commercially available, so this approach can involve a synthetic capability that many experimentalists do not possess.

Even if the disordered phase can be accessed, experiments in copolymer melts aimed at studying the MST are frequently plagued with the problem of achieving equilibrium. At the MST the mechanical properties of a copolymer melt change from those of a viscoelastic fluid in the disordered phase to those of a weakly bound elastic solid in the various ordered phases. It is not clear that a copolymer melt, on lowering the temperature from DIS,

will find the microphase morphology with the lowest free energy. One might expect that the system could become frozen into one of a variety of metastable structures. Indeed, micrographs of systems prepared in such a fashion exhibit large numbers of topological defects, such as grain boundaries and dislocations. It seems possible that, in addition to such defects, a copolymer melt could become locked into a nonoptimal periodic structure (e.g., LAM in place of HEX) because of peculiarities of the preparation procedure or merely because such a structure might be formed more rapidly than the lowest energy morphology. Even if the optimal structure is attained at the MST, it is possible that on further lowering the temperature the transitions predicted in ref 10 and 13 between different ordered structures would not be observed for kinetic reasons; namely, the system might become locked in the MST structure because the free energy barrier leading to the most stable structure is too large to surmount.

It was recognized years ago that many of these experimental difficulties are greatly alleviated when a solvent component is added to the melt. If the solvent is selective for one of the components of the copolymer, then the solution can have an extremely complicated phase diagram (including micellar phases) that may differ entirely from that of the pure melt. However, if the solvent is a good solvent of roughly equal affinity for all of the blocks, one expects that the copolymer solution will have thermodynamics similar to that of the pure melt. Furthermore, in such a solution equilibrium is more easily attained than in the melt and, because the unfavorable interactions among the blocks are diluted by the solvent, the MST and DIS phase can be more easily accessed for copolymers of reasonable molecular weight. The use of such *nonselective* (or neutral) solvents to study the MST has been exploited by various experimental groups, most recently by Hashimoto and co-workers[17-19] and Williams and co-workers.[20-22]

In order to interpret such experiments in block copolymer solutions, however, one needs to understand how the molten state theories are to be modified by the addition of a nonselective solvent. The usual approach[17-24] is to adopt the "dilution approximation", which states that the phase diagram of a neutral copolymer solution can be obtained from the corresponding melt phase diagram by replacing χ by $\phi\chi$, where ϕ is the polymer volume fraction in the solution. As we shall demonstrate later in the paper, such an approach neglects at least two elements of the physics of neutral copolymer solutions. The first is the neglect of excluded-volume interactions, which are clearly important in the semidilute regime. This is the experimentally relevant regime for studying the MST in most copolymer–solvent systems. The other difficulty with the dilution approximation is that it does not take account of inhomogeneities in solvent (and hence total polymer) concentration. We demonstrate below that (even in the weak segregation limit) *solvent inhomogeneities are always present in the ordered phases*. The physical mechanism leading to a nonuniform distribution of solvent is that an excess of solvent at the interfaces between microdomains can screen the energetically unfavorable A–B interactions at a small entropy cost and thereby lower the overall free energy.

A mean-field theory for neutral block copolymer solutions, more sophisticated than the dilution approximation, was developed by Noolandi and Hong (NH).[23] The theory requires detailed numerical calculations, and is thus difficult to employ, but it makes a number of interesting predictions. As with the dilution approximation, the NH theory neglects excluded-volume effects that are essential in the semidilute regime. Hence, its applicability is restricted to the concentration regime. Furthermore, the theory ignores the composition fluctuations that give rise to the FRH corrections discussed above. As a result, the approach is probably restricted to systems that are not too close to the MST (i.e., the strong segregation limit). In a subsequent paper,[24] NH expanded their free energy expression to treat the weak segregation limit, again neglecting Brazovskii fluctuation effects and excluded volume. Inhomogeneous solvent concentration profiles were incorporated (but, as we demonstrate in section II, not correctly). Phase diagrams were also generated for various model copolymer–solvent systems.

In the present paper we study the *weak segregation limit* of diblock copolymers in nonselective solvents that are *good* for both components of the diblock. We show how the random phase approximation can be extended to include solvent inhomogeneities and derive a Landau expansion for the free energy in terms of two coupled order parameters (section II). In section III the case of concentrated solutions is discussed and we provide both classical[10] and nonclassical[13] treatments of composition fluctuations. It is demonstrated that although the solvent concentration profiles in the ordered phases are nonuniform, the contributions of these nonuniformities to the free energy are very small if the neutral solvent is a good solvent. Furthermore, we show that the MST for a neutral block copolymer solution actually corresponds to a very narrow region of coexisting solvent-rich disordered and solvent-lean ordered phases. As a consequence of these observations, we find that the dilution approximation discussed above is an accurate approximation in the concentrated regime, provided it is used in conjunction with the nonclassical FRH phase diagram. Because the MST will occur in the semidilute regime for the majority of copolymer–solvent pairs, we also treat this regime in some detail (section IV), taking into account excluded-volume and nonclassical fluctuation effects. In addition to the phase diagram, we consider the scattering function of copolymer/neutral solvent mixtures. Section V contains a discussion of relevant experiments to test our predictions and suggests extensions of the present work.

II. Free Energy of Inhomogeneous Block Copolymer Solutions

In the present paper we consider solutions of A–B diblock copolymer dissolved in a nonselective, good solvent S. For simplicity, it is assumed that the solvent is athermal, hence the polymer–solvent interaction parameters satisfy $\chi_{AS} = \chi_{BS} = 0$, although our method requires only that the solvent be good. The polymers employed have N total statistical segments (monomers), each of length b, and the A block consists of Nf segments. We assume, in the spirit of a Flory–Huggins lattice model, that the monomers and solvent molecules have equivalent volumes, b^3, and we work in units of length such that b is unity. The Flory interaction parameter between A and B monomers is denoted χ, and ϕ is the average volume fraction of copolymer in the solution. In section IV we discuss the modifications of the above classical description that are required to treat the semidilute regime.

We assume incompressibility and zero volume change on mixing in the solution, hence the local volume fractions of monomer A, monomer B, and solvent must sum to unity. Equivalently, the fluctuations in these volume fractions must satisfy the sum rule, $\delta\phi_A(\mathbf{x}) + \delta\phi_B(\mathbf{x}) + \delta\phi_S(\mathbf{x}) = 0$. Thus, there are only two independent fluctuating fields, e.g., $\delta\phi_A(\mathbf{x})$ and $\delta\phi_B(\mathbf{x})$. The thermodynamic averages of these fields, $\langle\delta\phi_A(\mathbf{x})\rangle$ and $\langle\delta\phi_B(\mathbf{x})\rangle$, could be used as order

parameters to study the phase diagram of block copolymer solutions, but it is more convenient to define two new order parameters, ψ_1 and ψ_2, by means of the linear transformation

$$\psi_i(\mathbf{x}) = M_{ij}\langle\delta\phi_j(\mathbf{x})\rangle \tag{2.1}$$

with

$$\mathbf{M} = \phi^{-1}\begin{pmatrix} 1-f & -f \\ \phi & \phi \end{pmatrix} \tag{2.2}$$

and $\phi_1 \equiv \phi_A$, $\phi_2 \equiv \phi_B$. In eq 2.1 and in all subsequent equations, repeated indices imply a summation (Einstein convention). The order parameter $\psi_1(\mathbf{x})$ is the solution analogue of the order parameter $\psi(\mathbf{x})$ introduced by Leibler[10] for diblock melts. It is a finite amplitude, spatially periodic function if the copolymer solution is microphase separated, and vanishes identically in a homogeneous phase. In the limit that $\phi \to 1$, $\psi_1(\mathbf{x})$ reduces to the melt expression,[10] $\psi(\mathbf{x}) = \langle\delta\phi_A(\mathbf{x})\rangle$. The second-order parameter, $\psi_2(\mathbf{x}) = \langle\delta\phi_A(\mathbf{x})\rangle + \langle\delta\phi_B(\mathbf{x})\rangle$, describes the deviation of the polymer volume fraction from its average value ϕ. Hence, $\psi_2(\mathbf{x})$ is nonzero in situations where inhomogeneities in solvent concentration develop.

The phase diagram of diblock copolymer solutions in weakly inhomogeneous situations (i.e., the weak segregation limit) can be studied by deriving an expansion of the free energy in powers of the $\psi_i(\mathbf{x})$. The coefficients in such a Landau[26] expansion for a pure diblock melt have been evaluated by means of the random phase approximation (RPA).[10,27] The method can be extended in a straightforward manner to the present case of diblock solutions with two order parameters. However, some comments regarding such an extension are in order.

The RPA provides a classical treatment of concentration fluctuations and assumes Gaussian statistics, thereby neglecting excluded-volume swelling effects. Hence, it is strictly applicable only for concentrated solutions and for very large molecular weights. In the present section we give the results of applying the RPA method to diblock solutions. The resulting free energy expression is used in section III to analyze the phase diagram of high molecular weight, concentrated solutions, for which the theory is appropriate. We demonstrate there and in subsequent sections that the RPA results can be corrected to properly account for compositional order parameter fluctuations [i.e., fluctuations associated with the field $\psi_1(\mathbf{x})$] and excluded-volume effects by using the methods of FRH[13] and Broseta et al.[29]

The details of the RPA method, as applied to a diblock copolymer solution with two order parameters, are given in the Appendix. We obtain the following Landau expansion for the free energy density of a diblock copolymer in a nonselective, athermal solvent ($\beta = 1/k_BT$):

$$\beta F = \beta F_0 + \frac{1}{2!}V^{-2}\sum_{\mathbf{q}_1\mathbf{q}_2}\Gamma_{ij}^{(2)}(\mathbf{q}_1,\mathbf{q}_2)\psi_i(\mathbf{q}_1)\psi_j(\mathbf{q}_2) + \frac{1}{3!}V^{-3}\sum_{\mathbf{q}_1\mathbf{q}_2\mathbf{q}_3}\Gamma_{ijk}^{(3)}(\mathbf{q}_1,\mathbf{q}_2,\mathbf{q}_3)\psi_i(\mathbf{q}_1)\psi_j(\mathbf{q}_2)\psi_k(\mathbf{q}_3) + \frac{1}{4!}V^{-4}\sum_{\mathbf{q}_1\cdots\mathbf{q}_4}\Gamma_{ijkl}^{(4)}(\mathbf{q}_1,\mathbf{q}_2,\mathbf{q}_3,\mathbf{q}_4)\psi_i(\mathbf{q}_1)\psi_j(\mathbf{q}_2)\psi_k(\mathbf{q}_3)\psi_l(\mathbf{q}_4) \tag{2.3}$$

where V is the system volume and the Fourier transforms of the $\psi_i(\mathbf{x})$ are defined by

$$\psi_i(\mathbf{q}) = \int d\mathbf{x}\, \exp[i\mathbf{q}\cdot\mathbf{x}]\psi_i(\mathbf{x}) \tag{2.4}$$

The leading order term in eq 2.3 is the free energy density of a homogeneous block copolymer solution and is given by the simple Flory–Huggins expression

$$\beta F_0 = \frac{\phi}{N}\ln\phi + (1-\phi)\ln(1-\phi) + \chi f(1-f)\phi^2 \tag{2.5}$$

Note that no polymer–solvent interaction term appears in eq 2.5 because of the assumption of an athermal solvent.) The various vertex functions $\Gamma_{i_1\cdots i_n}^{(n)}(\mathbf{q}_1\cdots\mathbf{q}_n)$ appearing in eq 2.3 are related to correlation functions of noninteracting Gaussian chains as described in the Appendix. As in the pure melt case, $\Gamma_{ij}^{(2)}$ is temperature dependent through its dependence on χ. The higher order vertex functions, however, are temperature independent and are thus purely entropic in origin. Due to translational invariance of the solution, the $\Gamma_{i_1\cdots i_n}^{(n)}(\mathbf{q}_1\cdots\mathbf{q}_n)$ vanish unless $\sum_{i=1}^{n}\mathbf{q}_i = 0$. We exploit this to define

$$\Gamma_{ij}^{(2)}(\mathbf{q}_1,\mathbf{q}_2) = \delta^K(\mathbf{q}_1+\mathbf{q}_2)R_{ij}(\mathbf{q}_1) \tag{2.6}$$

where $\delta^K(\mathbf{q})$ is the Kronecker δ function. The explicit expressions for the $R_{ij}(q)$ are

$$R_{11}(q) = \phi[S(q)/W(q) - 2\chi\phi] \tag{2.7}$$

$$R_{12}(q) = R_{21}(q) = \{f[S_{12}(q)+S_{22}(q)] - (1-f)\times[S_{11}(q)+S_{12}(q)]\}[W(q)]^{-1} + \chi\phi(1-2f) \tag{2.8}$$

$$R_{22}(q) = [f^2S_{22}(q) - 2f(1-f)S_{12}(q) + (1-f)^2S_{11}(q)]/[\phi W(q)] + 2\chi f(1-f) + \upsilon \tag{2.9}$$

where $\upsilon = 1/(1-\phi)$ is the excluded-volume parameter. (Note that $\upsilon = 1/(1-\phi) - 2\chi_{PS}$ if the solvent is not athermal.) In the above equations, $S_{ij}(q) = V^{-1}\langle\delta\phi_i(\mathbf{q})\times\delta\phi_j(-\mathbf{q})\rangle$ is the matrix of correlation functions for a *melt* of noninteracting Gaussian diblock chains introduced in ref 10. The determinant of this matrix, $S_{11}S_{22} - S_{12}^2$, is denoted $W(q)$ and the sum of all the elements, $\sum_{ij}S_{ij}$, is denoted $S(q)$. The $S_{ij}(q)$ are given by[10]

$$S_{11}(q) = Ng_1(f,x) \tag{2.10}$$

$$S_{22}(q) = Ng_1(1-f,x) \tag{2.11}$$

$$S_{12} = S_{21} = \frac{1}{2}N[g_1(1,x) - g_1(f,x) - g_1(1-f,x)] \tag{2.12}$$

where

$$x \equiv q^2Nb^2/6 = q^2R_g^2 \tag{2.13}$$

(R_g is the radius of gyration) and where $g_1(f,x)$ is the modified Debye function

$$g_1(f,x) = 2[fx + \exp(-fx) - 1]/x^2 \tag{2.14}$$

The expression for the higher order vertex functions are shown in the Appendix to be given by

$$\Gamma_{ijk}^{(3)}(\mathbf{q}_1,\mathbf{q}_2,\mathbf{q}_3) = -\phi G_{lmn}^{(3)}(\mathbf{q}_1,\mathbf{q}_2,\mathbf{q}_3)Q_{il}(\mathbf{q}_1)Q_{jm}(\mathbf{q}_2)Q_{kn}(\mathbf{q}_3) \tag{2.15}$$

$$\Gamma_{ijkl}^{(4)}(\mathbf{q}_1,\mathbf{q}_2,\mathbf{q}_3,\mathbf{q}_4) = \phi\{V^{-1}\sum_{\mathbf{q}_5}S_{oq}^{-1}(\mathbf{q}_5)[G_{mno}^{(3)}(\mathbf{q}_1,\mathbf{q}_2,\mathbf{q}_5)G_{qpr}^{(3)}(-\mathbf{q}_5,\mathbf{q}_3,\mathbf{q}_4) + G_{mpo}^{(3)}(\mathbf{q}_1,\mathbf{q}_3,\mathbf{q}_5)G_{qnr}^{(3)}(-\mathbf{q}_5,\mathbf{q}_2,\mathbf{q}_4) + G_{mro}^{(3)}(\mathbf{q}_1,\mathbf{q}_4,\mathbf{q}_5)G_{qpn}^{(3)}(-\mathbf{q}_5,\mathbf{q}_3,\mathbf{q}_2)] - G_{mnpr}^{(4)}(\mathbf{q}_1,\mathbf{q}_2,\mathbf{q}_3,\mathbf{q}_4)\}Q_{im}(\mathbf{q}_1)Q_{jn}(\mathbf{q}_2)Q_{kp}(\mathbf{q}_3)Q_{lr}(\mathbf{q}_4) \tag{2.16}$$

In these expressions, $S_{ij}^{-1}(q)$ is the ijth element of the inverse of the matrix $\mathbf{S}(q)$ defined in eq 2.10–2.12. The matrix $Q_{ij}(q)$ is related to the $S_{ij}^{-1}(q)$ by

$$Q_{11}(q) = S_{11}^{-1}(q) - S_{12}^{-1}(q) \tag{2.17}$$

$$Q_{12}(q) = S_{12}^{-1}(q) - S_{22}^{-1}(q) \tag{2.18}$$

$$Q_{21}(q) = \phi^{-1}[fS_{11}^{-1}(q) + (1-f)S_{12}^{-1}(q)] \quad (2.19)$$

$$Q_{22}(q) = \phi^{-1}[fS_{12}^{-1}(q) + (1-f)S_{22}^{-1}(q)] \quad (2.20)$$

Finally, $G_{ijk}^{(3)}$ and $G_{ijkl}^{(4)}$ are the third- and fourth-order correlation functions for a *melt of noninteracting* Gaussian copolymer chains and are defined and evaluated in Appendices B and C of ref 10.

Certain tensorial elements of eq 2.15 and 2.16 are similar to the corresponding vertex function expressions for a diblock melt. It is easily seen that the particular diagonal elements $\Gamma_{111}^{(3)}$ and $\Gamma_{1111}^{(4)}$ are related to the melt expressions[10] Γ_3 and Γ_4 by a trivial factor of polymer volume fraction

$$\Gamma_{111}^{(3)}(\mathbf{q}_1,\mathbf{q}_2,\mathbf{q}_3) = \phi\Gamma_3(\mathbf{q}_1,\mathbf{q}_2,\mathbf{q}_3) \quad (2.21)$$

$$\Gamma_{1111}^{(4)}(\mathbf{q}_1,\mathbf{q}_2,\mathbf{q}_3,\mathbf{q}_4) = \phi\Gamma_4(\mathbf{q}_1,\mathbf{q}_2,\mathbf{q}_3,\mathbf{q}_4) \quad (2.22)$$

Similarly, $\Gamma_{11}^{(2)}(\mathbf{q}_1,\mathbf{q}_2)$ in eq 2.6, 2.7 is related to $\Gamma_2(\mathbf{q}_1,\mathbf{q}_2)$ of ref 10 by a factor of ϕ and by the replacement of χ by $\phi\chi$

$$\Gamma_{11}^{(2)}(\mathbf{q}_1,\mathbf{q}_2) = \phi\Gamma_2(\mathbf{q}_1,\mathbf{q}_2)|_{\chi\to\phi\chi} \quad (2.23)$$

However, the remaining elements of the vertex function tensors for a neutral diblock solution are new and reflect the physics of coupling to solvent inhomogeneities through the second-order parameter $\psi_2(\mathbf{q})$.

A comment about the ϕ-dependence of the free energy expression 2.3 is appropriate. For a system exhibiting a single thermodynamic phase, the definitions given for the $\psi_i(\mathbf{q})$ in eq 2.1 imply that their $\mathbf{q} = 0$ components must vanish. For an equilibrium system that has two coexisting phases α and β with average polymer volume fractions ϕ^α and ϕ^β, respectively, $\psi_2(\mathbf{q})$ will in general have a nonzero $\mathbf{q} = 0$ component. However, when evaluating the free energy density expression 2.3 for a phase α, if we interpret ϕ in eq 2.3 as the average volume fraction of polymer in that phase, ϕ^α, then the $\mathbf{q} = 0$ component of $\psi_2(\mathbf{q})$ can be made to vanish. We adopt this interpretation of ϕ in the subsequent analysis.

Having completed the specification of the terms in the free energy, eq 2.3, we begin its analysis. To simplify the presentation, we initially restrict consideration to the special case of *symmetric* copolymers with $f = {}^1/_2$ and to the *lamellar* microphase morphology. The results are subsequently generalized to the asymmetric case and to other morphologies.

The linear stability of a homogeneous block copolymer solution to fluctuations in A–B composition or solvent concentration is related to the sign of the determinant of the matrix $\mathbf{R}(q)$, defined in eq 2.7–2.9 It follows from eq 2.8 and 2.10–2.12 that $\mathbf{R}(q)$ is diagonal in the symmetric case and its determinant is simply

$$\Delta(q) = \phi[S(q)/W(q) - 2\chi\phi]\{[\phi N g_1(1,x)]^{-1} + \chi/2 + v\} \quad (2.24)$$

The third factor in this expression is positive and of order unity for athermal solvents; hence the zero of the second factor determines the stability limit of a homogeneous phase, i.e., the spinodal. The quantity $S(q)/W(q)$ in that factor is minimized by a particular wavenumber $q^* = q^*(f)$. The minimum value $2\kappa/N \equiv S(q^*)/W(q^*)$ corresponds to $2\chi_s\phi_s$, twice the product of χ and ϕ at the spinodal. The functions $\kappa = \kappa(f)$ and $x^* \equiv (q^*R_g)^2 = x^*(f)$ are smooth functions of copolymer composition that are tabulated in FRH[13] and in Table I. (In the notation of ref 10, $\kappa \equiv \chi_s N$.) For symmetric copolymers they assume the values $\kappa(0.5) = 10.495$ and $x^*(0.5) = 3.7852$. Because $x^* > 0$, it is apparent that the spinodal instability is to a spatially inhomogeneous microphase pattern.

Table I
Some Composition-Dependent Coefficients[a]

f	x^*	κ	H	π_1
0.50	3.7852	10.495	8.1058	48.694
0.45	3.7995	10.698	8.1346	49.603
0.40	3.8433	11.344	8.2233	52.493
0.35	3.9207	12.562	8.3799	57.928
0.30	4.0395	14.635	8.6203	67.148
0.25	4.2138	18.172	8.9733	82.806
0.20	4.4708	24.613	9.4938	111.14
0.15	4.8676	38.038	10.297	169.72
0.10	5.5517	74.331	11.683	326.35
0.05	7.1091	255.85	14.830	1097.1

[a] Various composition-dependent coefficients that are required to evaluate the free energy in eq 2.39. The general coefficient $C(f)$ has the symmetry property $C(f) = C(1-f)$.

To analyze the phase diagram of diblock copolymer solutions in the weak segregation limit, we assume[10,13,26] that the inhomogeneous A–B patterns (mesophases) formed near the stability limit consist of superpositions of plane waves with wavenumber q^*, i.e., those having the largest growth rate from the homogeneous phase.[30] Thus, we assume the following representation for the compositional order parameter $\psi_1(\mathbf{x})$

$$\psi_1(\mathbf{x}) = A_n n^{-1/2}\sum_{k=1}^{n}\{\exp[i(\mathbf{Q}_k\cdot\mathbf{x} + \delta_k)] + \text{c.c.}\} \quad (2.25)$$

where c.c. represents the complex conjugate and the $\{\mathbf{Q}_k\}$ are a set of n reciprocal lattice vectors with equal magnitudes $|\mathbf{Q}_k| = q^*$ that span the microphase morphology of interest.[10] The phases, δ_k, and the amplitude, A_n, are to be determined by minimization of the free energy expression, eq 2.3. For the present analysis of a lamellar pattern, $n = 1$, eq 2.25 reduces to $\psi_1(\mathbf{x}) = 2A_1\cos[\mathbf{Q}_1\cdot\mathbf{x} + \delta_1]$.

By substituting eq 2.25 into eq 2.3, various types of couplings arise between the assumed form for ψ_1 and the (as yet) unparameterized ψ_2. For the symmetric case there are no quadratic couplings and the cubic term in eq 2.3 gives the lowest order coupling between the two fields. In particular, this coupling term is

$$I = \frac{1}{3!}V^{-3}\sum_{\mathbf{q}_1\mathbf{q}_2\mathbf{q}_3}\{\Gamma_{211}^{(3)}(\mathbf{q}_1,\mathbf{q}_2,\mathbf{q}_3)\psi_2(\mathbf{q}_1)\psi_1(\mathbf{q}_2)\psi_1(\mathbf{q}_3) + \Gamma_{121}^{(3)}(\mathbf{q}_1,\mathbf{q}_2,\mathbf{q}_3)\psi_1(\mathbf{q}_1)\psi_2(\mathbf{q}_2)\psi_1(\mathbf{q}_3) + \Gamma_{112}^{(3)}(\mathbf{q}_1,\mathbf{q}_2,\mathbf{q}_3)\psi_1(\mathbf{q}_1)\psi_1(\mathbf{q}_2)\psi_2(\mathbf{q}_3)\} \quad (2.26)$$

The translational invariance property of $\Gamma_{ijk}^{(3)}$ and eq 2.25 implies that eq 2.26 gives a nonvanishing contribution to the free energy if $\psi_2(\mathbf{x})$ has the following form

$$\psi_2(\mathbf{x}) = B_n n^{-1/2}\sum_{k=1}^{n}\sum_{l=1}^{n}\{\exp[i(\mathbf{x}\cdot[\mathbf{Q}_k + \mathbf{Q}_l] + \mu_{kl})] + \text{c.c.}\} + C_n n^{-1/2}\sum_{k=1}^{n}\sum_{l=1}^{n}\{\exp[i(\mathbf{x}\cdot[\mathbf{Q}_k - \mathbf{Q}_l] + \tau_{kl})] + \text{c.c.}\} \quad (2.27)$$

where B_n and C_n are arbitrary amplitudes and μ_{kl} and τ_{kl} arbitrary phases. (One could write a more general expression in which B_n and C_n depend on k and l, but this proves unnecessary for the present study.) For the case of lamellae ($n = 1$), eq 2.27 simplifies to

$$\psi_2(\mathbf{x}) = 2B_1\cos[2\mathbf{Q}_1\cdot\mathbf{x} + \mu_{11}] \quad (2.28)$$

The absence of a term proportional to C_1 is a consequence of $\psi_2(\mathbf{q}=0) = 0$, as discussed above. Thus, the lowest order cubic coupling for a lamellar phase suggests that if inhomogeneities in solvent concentration develop, they will be characterized by a wavenumber of $2q^*$. This choice of

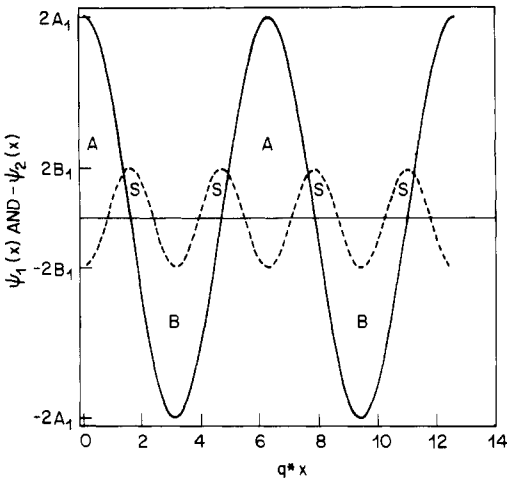

Figure 2. Schematic of the profiles of solvent concentration (dashed), $\langle \delta\phi_S(x) \rangle = -\psi_2(x)$, and A–B compositional order parameter (solid), $\psi_1(x) = \phi^{-1}[(1-f)\langle \delta\phi_A(x) \rangle - f\langle \delta\phi_B(x) \rangle]$, for the lamellar microphase of a diblock copolymer in a good, nonselective solvent. The solvent profile has a period of π/q^*, while the compositional order parameter $\psi_1(x)$ has twice that period. As the figure indicates, the maxima in solvent concentration correspond to the (interfacial) nodal points where $\psi_1(x)$ vanishes; i.e., the points that separate A-rich from B-rich domains.

wavenumber is also the physically motivated one, because (with an appropriate choice of the phase μ_{11}) it allows excess solvent to be present at all the nodal planes that separate regions of the solution having an excess of A or B, respectively (see Figure 2). Such placement of the solvent can partially screen the unfavorable A–B interactions. It remains to be seen whether the enthalpic benefits of nonuniform solvent profiles can outweigh the entropy penalties associated with the creation of such profiles.

Continuing with our analysis of lamellar patterns and symmetric copolymers, we substitute the above parameterization of $\psi_2(\mathbf{x})$ and eq 2.25 (for $n = 1$) into the free energy expression (2.3). A large number of terms results, each of which is a polynomial in A_1 and B_1 of total order at least two. For the purpose of studying the weak segregation limit and good solvents, it is sufficient to retain terms only to fourth order in A_1. An enormous simplification occurs in the present problem, because it turns out that the B_1's which minimize the free energy are of order A_1^2. (This claim is substantiated later.) Hence, the only terms involving B_1 that need be retained in the series emerging from eq 2.3 are of order B_1^2 and $B_1A_1^2$.

The terms in eq 2.3 that are of order B_1^2 arise from the quadratic free energy contribution

$$\mathrm{II} = \frac{1}{2!}V^{-2}\sum_{\mathbf{q}_1\mathbf{q}_2}\Gamma_{22}^{(2)}(\mathbf{q}_1,\mathbf{q}_2)\psi_2(\mathbf{q}_1)\psi_2(\mathbf{q}_2) \qquad (2.29)$$

Making use of eq 2.6 and 2.9 and inserting eq 2.28, this expression becomes

$$\mathrm{II} = [H(f)/N\phi + 2\chi f(1-f) + v]B_1^2 \qquad (2.30)$$

where

$$H(f) \equiv N[f^2S_{11}^{-1}(2q^*) + 2f(1-f)S_{12}^{-1}(2q^*) + (1-f)^2S_{22}^{-1}(2q^*)] \qquad (2.31)$$

The contribution of order $B_1A_1^2$ is that arising from the cubic free energy terms I, given in eq 2.26. On insertion of eq 2.25 and 2.28, one obtains

$$\mathrm{I} = -\frac{\pi_1}{N}\cos(2\delta_1 - \mu_{11})B_1A_1^2 \qquad (2.32)$$

where

$$\pi_1 = -\frac{N}{3}[\Gamma_{211}^{(3)}(1) + \Gamma_{121}^{(3)}(1) + \Gamma_{112}^{(3)}(4)] \qquad (2.33)$$

In eq 2.33 we employ the notation of ref 10, in which $\Gamma_{ijk}^{(3)}(\mathbf{q}_1,\mathbf{q}_2,\mathbf{q}_3)$ for $\mathbf{q}_1 + \mathbf{q}_2 + \mathbf{q}_3 = 0$ is denoted $\Gamma_{ijk}^{(3)}(h)$, where $|\mathbf{q}_1 + \mathbf{q}_2|^2 = |\mathbf{q}_3|^2 = h(q^*)^2$. By substitution of eq 2.15 and use of eq 2.17–2.20, $\pi_1 = \pi_1(f)$ can be written as

$$\pi_1 = \frac{N}{3}[G_{rpq}^{(3)}(1)[S_{q1}^{-1} - S_{q2}^{-1}]\{[S_{p1}^{-1} - S_{p2}^{-1}][fS_{r1}^{-1}(2q^*) + (1-f)S_{r2}^{-1}(2q^*)] + [S_{r1}^{-1} - S_{r2}^{-1}][fS_{p1}^{-1}(2q^*) + (1-f)S_{p2}^{-1}(2q^*)]\} + G_{rpq}^{(3)}(4)[S_{r1}^{-1} - S_{r2}^{-1}] \times [S_{p1}^{-1} - S_{p2}^{-1}][fS_{q1}^{-1}(2q^*) + (1-f)S_{q2}^{-1}(2q^*)]] \qquad (2.34)$$

where the $G_{ijk}^{(3)}(h)$ are given in Appendix C of ref 10 and where S_{ij}^{-1} represents $S_{ij}^{-1}(q^*)$.

The free energy contributions I and II contain two functions, $H(f)$ and $\pi_1(f)$, that depend on the copolymer composition, f, but are independent of molecular weight and average polymer concentration. Values of these functions at various compositions are given in Table I. Because $\pi_1 > 0$ for $f = {}^1/_2$ and (to fourth order in A_1) the phase μ_{11} appears only in term I of the free energy, it follows from eq 2.32 that the total free energy is minimized by the choice of μ_{11} such that $\cos(2\delta_1 - \mu_{11}) = 1$. This choice of phase is consistent with the physical expectation that the solvent concentration should be maximum at the interfaces between A- and B-rich regions, i.e., at the points where $\psi_1(\mathbf{x})$ vanishes (see Figure 2). Equation 2.32 can now be rewritten as

$$\mathrm{I} = -\frac{\pi_1}{N}B_1A_1^2 \qquad (2.35)$$

Up to fourth order in A_1, the terms in the free energy other than I and II are independent of B_1. Because of the special properties of the diagonal vertex functions noted in eq 2.21–2.23, these remaining terms can be obtained from the free energy density computed in ref 10 for a pure diblock melt. Hence, combining results of ref 10 and the present expressions for I and II, the total free energy of a solution of symmetric copolymer in a nonselective, athermal solvent can be written

$$\beta F = \beta F_0 + \frac{\phi}{N}\{2(\kappa - \phi\chi N)A_1^2 - \alpha_1A_1^3 + \beta_1A_1^4\} + [H(f)/N\phi + 2\chi f(1-f) + v]B_1^2 - \frac{\pi_1}{N}B_1A_1^2 \qquad (2.36)$$

The coefficients α_1 and β_1 were computed in ref 10 and depend only on the copolymer composition, f. The coefficients $\kappa(f)$, $H(f)$, and $\pi_1(f)$ are given for various compositions in Table I.

Minimization of eq 2.36 with respect to the amplitude B_1 leads to the relationship

$$B_1 = \frac{\pi_1\phi}{2p(f,\phi)}A_1^2 \qquad (2.37)$$

where

$$p(f,\phi) \equiv H(f) + 2\chi Nf(1-f)\phi + vN\phi \qquad (2.38)$$

Equation 2.37 confirms that B_1 is of order A_1^2 and justifies the neglect of higher order free energy terms. It also indicates that *inhomogeneities in solvent concentration will be present for any nonzero A_1, i.e., whenever the solution is microphase separated.* This result was not obtained by Hong and Noolandi[24] in their analysis of the weak segregation limit of block copolymer solutions. The discrepancy emerges from an incorrect description of the solvent con-

centration field in ref 24. In particular, Hong and Noolandi characterized inhomogeneous solvent patterns as superpositions of plane waves with wave vectors of magnitude q^*, instead of the demonstrated and physically motivated choice $2q^*$ employed in eq 2.28. As illustrated in Figure 2, the correct solvent concentration profile for a lamellar morphology is out of phase with and has a period half that of the A–B composition profile.

The free energy at the extremal B_1 follows from eq 2.36 and 2.37

$$\beta F = \beta F_0 + \frac{\phi}{N}\left\{2(\kappa - \phi\chi N)A_1^2 - \alpha_1 A_1^3 + \left[\beta_1 - \frac{\pi_1^2}{4p(f,\phi)}\right]A_1^4\right\} \quad (2.39)$$

We emphasize that this classical RPA result is valid only for concentrated solutions and at high molecular weight. Under such conditions and for an athermal (or good) solvent, the first two terms in eq 2.38 for $p(f,\phi)$ are of order unity near the MST. However, the third term in eq 2.38, $\upsilon N\phi$, is $O(N)$ under the same conditions. It follows from eq 2.37 that the amplitudes of the solvent inhomogeneities are smaller by N^{-1} than those of the A–B patterns and that the term proportional to π_1^2 in the free energy expression (2.39) is negligible compared with β_1. Dropping this term in eq 2.39, we recover the familiar dilution approximation[17-24] for the free energy. To our knowledge this is the first derivation of the dilution approximation that convincingly justifies the neglect of contributions from solvent inhomogeneities to the free energy of concentrated block copolymer solutions with nonselective, good solvents. Although inhomogeneous solvent patterns may not contribute to the free energy, our derivation shows that they are always present in the microphase-separated state and, thus, might be detected in scattering experiments.

The above arguments leading to eq 2.39 for lamellar patterns and symmetric copolymers can be repeated for more complicated morphologies and arbitrary asymmetry. We again find that for good, nonselective solvents (and within the classical RPA) nonuniform solvent concentration profiles contribute negligibly to the free energy. Thus, we can generalize our above results to obtain a very simple and intuitive expression (i.e., the dilution approximation) for the free energy (per lattice site of volume $b^3 = 1$) of a neutral, athermal copolymer solution

$$\beta F(\phi,A_n) = \frac{\phi}{N}\ln\phi + (1-\phi)\ln(1-\phi) + \chi f(1-f)\phi^2 + \frac{\phi}{N}[2(\kappa - \phi\chi N)A_n^2 - \alpha_n A_n^3 + \beta_n A_n^4] \quad (2.40)$$

where the coefficients α_n and β_n for $n \geq 1$ are given in ref 10. The first two terms in this expression are the usual Flory contributions to the entropy of mixing polymer and solvent. The third term is enthalpic, arising from A–B interactions. The final term (in square brackets), which vanishes for a compositionally disordered copolymer solution, describes the extra contribution to the free energy arising from inhomogeneities in A and B monomer density. It differs from the free energy expression obtained by Leibler[10] for a diblock melt only by the leading factor of ϕ and by classical dilution of the A–B interactions, i.e., replacement of χ by $\phi\chi$. Because solvent nonuniformities are neglected, the inhomogeneous term in the free energy is simply weighted by the average volume fraction of copolymer in the solution.

It is important to emphasize that the above results are based on the assumption that the solvent is good (indeed, athermal) for both components of the diblock. If the solvent is marginal or poor, such that $\upsilon N\phi$ is of order unity, then the solvent inhomogeneities are much more important. We consider this case in a future publication.[31]

III. Concentrated Regime

We now analyze the phase diagram for concentrated solutions of A–B diblock copolymer in a nonselective, athermal solvent. Because the volume fraction of copolymer, ϕ, is large in the concentrated regime, excluded-volume effects can be neglected. Initially, we also neglect the effects of A–B composition fluctuations treated by FRH[13] and work at the mean-field level of the previous section.

To locate the MST on the basis of eq 2.40 the free energy is to be minimized with respect to the amplitude A_n. Moreover, because the system has two components, copolymer and solvent, we search for two-phase coexistence by equating chemical potentials of solvent-rich disordered and solvent-poor ordered phases. Equation 2.40 is minimized (for an ordered phase) by the choice of amplitude $A_n = \bar{A}_n$, where

$$\bar{A}_n = 3\alpha_n(1+\gamma_n)/8\beta_n \quad (3.1)$$

$$\gamma_n \equiv [1 - 64\beta_n(\kappa - \phi\chi N)/9\alpha_n^2]^{1/2} \quad (3.2)$$

With this amplitude and for fixed temperature, molecular weight, and copolymer composition, the inhomogeneous term in eq 2.40 (the last term) vanishes at a polymer volume fraction ϕ_0. This critical volume fraction satisfies the equation

$$\kappa - \phi_0\chi N = \alpha_n^2/8\beta_n \quad (3.3)$$

and at $\phi = \phi_0$, the amplitude reduces to $\bar{A}_n \equiv S_n = \alpha_n/2\beta_n$. Anticipating that the polymer volume fractions in the two coexisting phases at the MST will lie close to ϕ_0, we expand eq 2.40 (for an ordered phase) about ϕ_0 to obtain ($\phi = \phi_0 + \delta\phi$)

$$\beta F_{ord} = \beta F_{00} + A\delta\phi + B\delta\phi^2 + \ldots \quad (3.4)$$

with

$$\beta F_{00} = \frac{\phi_0}{N}\ln\phi_0 + (1-\phi_0)\ln(1-\phi_0) + \chi f(1-f)\phi_0^2 \quad (3.5)$$

$$A = -[1 + \ln(1-\phi_0) - 2\chi f(1-f)\phi_0 + 2\chi\phi_0 S_n^2] \quad (3.6)$$

$$B = 1/[2(1-\phi_0)] + \chi f(1-f) - 2\chi S_n^2 - 4\phi_0\chi^2 N/\beta_n \quad (3.7)$$

The corresponding expansion of the free energy for a compositionally disordered phase is

$$\beta F_{dis} = \beta F_{00} + A'\delta\phi + B'\delta\phi^2 + \ldots \quad (3.8)$$

with

$$A' = -[1 + \ln(1-\phi_0) - 2\chi f(1-f)\phi_0] \quad (3.9)$$

$$B' = 1/[2(1-\phi_0)] + \chi f(1-f) \quad (3.10)$$

Next, we equate chemical potentials, $\mu = \beta\partial F/\partial\phi$, and osmotic pressures, $\Pi = \phi\mu - \beta F$, of the ordered and disordered phases to determine the polymer concentrations, ϕ_+ and ϕ_-, of the coexisting polymer-rich and polymer-lean phases. We find from eq 3.4 and 3.8 that to leading order

$$\delta\phi_+ = \frac{A' - A}{2[B + (BB')^{1/2}]} \quad (3.11)$$

$$\delta\phi_- = \frac{A - A'}{2[B' + (BB')^{1/2}]} \quad (3.12)$$

For the present concentrated regime in which $1 - \phi_0 \ll 1$, eq 3.11 and 3.12 reduce to

$$\frac{\delta\phi_+}{\phi_0} \approx -\frac{\delta\phi_-}{\phi_0} \approx (1 - \phi_0)\chi S_n^2 \tag{3.13}$$

The above results, in conjunction with the numerical data[10,13] for κ, α_n, and β_n, indicate that the total free energy in the vicinity of the MST is minimized for *asymmetric* copolymers ($f \neq {}^1/_2$) by a coexistence between a solvent-rich disordered phase and a solvent-lean BCC phase ($n = 6$). However, for perfectly *symmetric* copolymer solutions, as in Leibler's theory for the pure melt, we find that the LAM phase is lower in free energy and thus predict LAM–DIS coexistence. For the asymmetric case it follows from eq 3.13 that the width of the coexistence region is

$$(\phi_+ - \phi_-)/\phi_0 \approx 2(1 - \phi_0)\chi S_6^2 \tag{3.14}$$

This expression, however, is extremely small as a consequence of the smallness of each of the three factors. The first, $1 - \phi_0$, is necessarily small because of our restriction to the concentrated regime. The Flory interaction parameter χ is typically $O(10^{-1})$ for highly incompatible blocks, while for less incompatible blocks, such as isomeric pairs[11,16] or isotopic pairs,[25] χ is usually $O(10^{-2})$ to $O(10^{-4})$. Numerical evaluation of the third factor, $S_6 = \alpha_6/2\beta_6$, shows it to be very small as well. This amplitude vanishes asymptotically in the limits $f \to 0$ and $f \to 1$ and at $f = {}^1/_2$. At the intermediate compositions of 0.25 and 0.75, S_6 assumes the value 0.045. Our prediction, then is that the two-phase BCC–DIS coexistence region for a concentrated solution with a good, nonselective solvent will be extremely narrow, probably imperceptible from an experimental standpoint.

For the case of a perfectly symmetric copolymer in a neutral solvent, the width of the LAM–DIS coexistence region actually vanishes because $S_1 = 0$. Hence, the symmetric MST in the present mean-field theory is predicted to be sharp and continuous, as in the pure melt. Absence of a two-phase region at the MST for a copolymer solution is permitted only if the transition is second order, as at $f = {}^1/_2$. For two-component systems exhibiting a first-order transition of the order–disorder type, a two-phase coexistence region must separate the phases with different symmetry.[26] This is consistent with the above results for asymmetric diblock solutions. Finally, we comment that Hong and Noolandi[24] in their treatment of concentrated copolymer solutions performed calculations primarily for the symmetric case. Because their theory is of the same mean-field type as that just described and leads to a second-order transition, they found no two-phase region at the MST. (However, they did find an unrelated two-phase region at very low temperatures that arises from the fact that the solvents they employed were not sufficiently good to maintain a mixed phase.)

Because the coexistence region at the MST is found to be so narrow, for all practical purposes one can locate the transition by using eq 3.3 for $n = 6$. We note that eq 3.3 is obtained from a similar expression derived in ref 10 for pure copolymer melts by the replacement of χ by $\phi\chi$. Since κ and $\alpha_6^2/8\beta_6$ depend only on copolymer composition, f, eq 3.3 predicts that the critical polymer concentration at the MST scales with molecular weight as $\phi_t \sim N^{-1}$.

One can also use eqs 3.4–3.7 to study coexistence between two (different) compositionally ordered phases in the weak segregation limit. The expansion is still legitimate for this case because, as found in ref 10, the lines of mesophase coexistence lie very close to the MST. The result of analyzing coexistence between two ordered phases (for a concentrated solution of diblock copolymer in a neutral, athermal solvent) is again that the two-phase region is very narrow. This result and those for the location of the MST indicate that we can obtain a reasonable approximation for the phase diagram of a concentrated copolymer solution (in mean-field theory) by merely replacing χ by $\phi\chi$ in the phase diagram generated for diblock melts by Leibler.[10] Hence, we provide theoretical justification for the dilution approximation.[17-24] Figure 1 shows this mean-field prediction for the phase diagram.

Although excluded-volume interactions are screened in a concentrated diblock solution, fluctuations in A–B composition with wavelengths $2\pi/q^*$ (of order the radius of gyration) become coherent over large distances as the MST is approached, particularly for symmetric copolymers. Hence, the Brazovskii fluctuation corrections introduced for diblock melts by FRH[13] should also be taken into account for the present problem. To incorporate such corrections we employ the following free energy expression in place of eq 2.40:

$$\beta F(\phi,a_n) = \frac{\phi}{N}\ln\phi + (1-\phi)\ln(1-\phi) + \chi f(1-f)\phi^2 + \frac{\phi}{N}\left[\frac{1}{2\lambda}(r^2 - r_0^2)\frac{d}{N^{1/2}}(r^{1/2} - r_0^{1/2}) - \frac{2}{3}n\theta_n a_n^3 + \frac{1}{2}n\eta_n a_n^4\right] \tag{3.15}$$

where the free energy density of a diblock melt obtained in ref 13 has been substituted (in the dilution approximation) for that of Leibler. Note that $\bar{N} = N$ is the present (lattice) theory.[32] In eq 3.15, λ and d are f-dependent coefficients that are defined and tabulated in ref 13 and a_n is an amplitude similar to A_n. The coefficients θ_n and η_n are also defined in FRH and are related to Leibler's coefficients α_n and β_n discussed above. The self-consistent Hartree approximations for the inverse susceptibilities of the disordered phase, r_0, and ordered phase, r, satisfy the algebraic equations[13]

$$r_0 = \tau + d\lambda/(r_0 N)^{1/2} \tag{3.16}$$

$$r = \tau + d\lambda/(rN)^{1/2} + n\lambda a_n^2 \tag{3.17}$$

where

$$\tau = 2(\kappa - \phi\chi N)/c^2 \tag{3.18}$$

with c an f-dependent constant defined in FRH. The free energy, eq 3.15, is minimized by the amplitude $a_n = \bar{a}_n$, which satisfies the equation

$$\eta_n \bar{a}_n^2 - \theta_n \bar{a}_n + r = 0 \tag{3.19}$$

Analysis of the free energy expression (3.15) by the method used to treat eq 2.40 leads to results similar to those obtained above. The width of the two-phase region at the MST is again so narrow that it can be safely ignored. However, we comment that the Hartree approximation leads to a first-order transition at all copolymer compositions; hence a narrow two-phase region is found even for a symmetric copolymer. For this special case of $f = {}^1/_2$ the MST is predicted by eq 3.15 to occur at $(\phi\chi N)_t = 10.495 + 41.022\,N^{-1/3}$. As before, the phase diagram for a concentrated solution can be obtained from the melt phase diagram by the replacement of χ by $\phi\chi$. In Figure 3 we show a phase diagram calculated in the Hartree approximation for a concentrated solution with $N = 10^6$.

Although the equations given above possess solutions for low molecular weight, we only believe them to be accurate at very large N. (See the discussion in FRH.[13]) In the limit of infinite molecular weight, composition fluc-

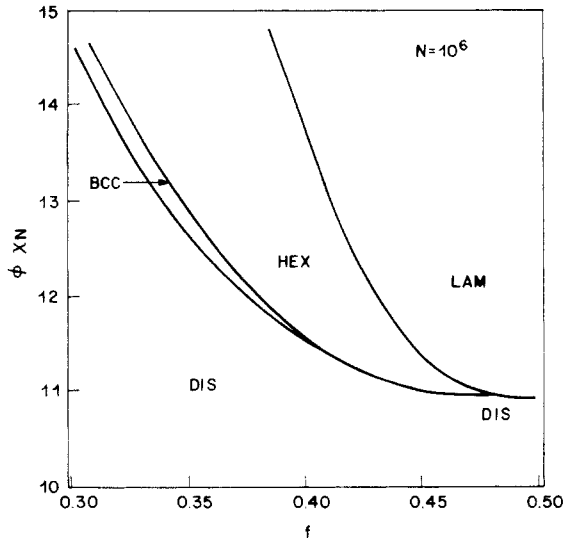

Figure 3. Phase diagram for a concentrated diblock solution with a good, nonselective solvent in the self-consistent Hartree approximation. The diagram shown is for copolymer molecules with degree of polymerization $N = 10^6$. In the limit $\phi \to 1$ the figure reduces to a phase diagram derived for a copolymer melt in ref 13. The phase diagram for a semidilute solution with $Z = 10^6$ blobs per molecule is obtained from the present figure by relabeling the ordinate to $\chi_{eff}Z$.

tuations are suppressed and eq 3.15 reduces to the mean-field free energy expression given in eq 2.40. The results of Figure 1 are recovered in that limit. However, it is important to note that the phase diagram for a solution of hypothetical molecules with infinite molecular weight is *qualitatively* different than the corresponding phase diagram for a system with a very large, but finite, molecular weight.

Another useful result that emerges from the present theory is an expression for the disordered phase scattering function of a concentrated diblock copolymer solution. Depending on the method of labeling, neutron and X-ray scattering experiments can be used to probe various elements of $\mathbf{R}^{-1}(q)$, the inverse of the matrix $\mathbf{R}(q)$ given in eq 2.7–2.9. In an experiment where the contrast comes from fluctuations in A–B composition and where fluctuations in solvent concentration can be neglected, a great simplification is obtained. Namely, the intensity of scattered radiation depends only on the matrix element $R_{11}(q)$. This intensity is given in the Hartree approximation (for concentrated solutions with good, nonselective solvents) by (cf. eq 5.1 of ref 13)

$$I(q) = \phi^2\langle\psi_1(\mathbf{q})\psi_1(-\mathbf{q})\rangle = \frac{\phi N}{\epsilon + [F(q^2R_g^2,f) - 2\kappa]} \tag{3.20}$$

where $F(x,f) \equiv NS(q)/W(q)$ is a dimensionless $O(1)$ function whose explicit expression is given in eq IV-6 of ref 10 and $\epsilon = r_0c^2$ is the solution of the algebraic equation

$$\epsilon = 2\kappa - 2\phi\chi N + c^3d\lambda/(\epsilon N)^{1/2} \tag{3.21}$$

Scattering experiments could be used to confirm the form of eq 3.20 for concentrated solutions or as an independent means of determining χ. Other experiments that employ a different type of labeling, for example a deuteriated solvent,[36] could be used to test the ability of eq 2.7–2.9 to describe fluctuations in solvent concentration.

IV. Semidilute Regime

For the more common situation of strongly incompatible blocks, microphase separation in nonselective solvents is expected to take place in the semidilute regime.[28,29] In this regime chains interpenetrate quite extensively, but the total polymer volume fraction is ideally very small.[27] Furthermore, excluded-volume interactions are still important on distance scales less than ξ, the correlation length for segment (monomer) concentration fluctuations, but are screened out at distances larger than ξ. As the polymer concentration is increased, the screening becomes more pronounced and the correlation length decreases[27] like $\phi^{-\nu/(3\nu-1)} \sim \phi^{-0.77}$, where $\nu \approx 0.588$ is the excluded-volume exponent. Because of these excluded-volume effects at short distances, the probability of contact between two like segments has been shown[27,28] to be reduced by a factor of $\phi^{(2\nu-1)/(3\nu-1)} \sim \phi^{0.23}$. Recent renormalization group studies[28,33,34] have demonstrated that the probability of contacts between unlike segments is even further reduced by an additional factor of $\phi^{\chi_{SD}}$, where $\chi_{SD} \approx 0.29$ is a crossover exponent given by $\chi_{SD} = \chi_S/(3\nu - 1)$, with $\chi_S \approx 0.22$.

We begin our analysis of the semidilute regime with the ansatz that contributions to the free energy from nonuniform solvent concentration patterns are negligible. As we will show later, this assumption is legitimate for long copolymer chains [i.e., when $N^{-0.22} \ll O(1)$], in which case it permits a very simple theory for the phase diagram to be constructed. However, it is important to keep in mind that the solvent is always distributed nonuniformly in the various ordered phases, with a slight excess of solvent in the interfacial regions between microdomains. The free energy and phase diagram is not sensitive (at sufficiently high molecular weight) to this inhomogeneity, but certain experiments (such as scattering measurements involving labeled solvents) can directly probe solvent concentration fluctuations and patterns.

A standard procedure in semidilute polymer solutions is to group the monomers into[27] "blobs" of size the correlation length ξ. Each blob contains $g = \phi(\xi/b)^3$ monomers that are in general of the same chemical nature. For the present case of diblock copolymer solutions in nonselective solvents, each chain may be viewed as a diblock of blobs, with $n_A = Nf/g$ blobs of type A and $n_B = N(1-f)/g$ blobs of type B. Because excluded volume swelling is restricted to the interior of each blob, the solution is then equivalent to a melt of copolymers formed by these blobs. The calculations of ref 28 and 33–34 discussed above suggest that the interactions between A and B blobs may be described by an effective Flory parameter

$$\chi_{eff} = w\phi^{\chi_{SD}} \sim \phi^{0.29} \tag{4.1}$$

By exploiting a similar blob picture, Broseta, Leibler, and co-workers[29,35] have been able to make a number of interesting predictions for the critical properties of semidilute mixtures of homopolymers in nonselective solvents. These predictions appear to be in good agreement with the available experiments and simulations.

The above blob description is easily implemented for the case of a semidilute solution of diblock copolymer in a solvent in a solvent that is neutral and good for both components. If we work at a mean-field level in treating the A–B composition fluctuations, then by analogy with eq 2.40 for the concentrated regime, the appropriate expression for the free energy density of a semidilute solution is

$$\beta F(\phi,A_n) = \frac{1}{Z\xi^3}\{2[\kappa - \chi_{eff}Z]A_n^2 - \alpha_nA_n^3 + \beta_nA_n^4\} + K\xi^{-3} \tag{4.2}$$

In this equation $Z = n_A + n_B$ is the total number of blobs per copolymer chain and K is a universal constant[29] ≈ 0.02. The last term in eq 4.2 describes the asymptotic pair in-

teractions (at the semidilute fixed point) between all types of blobs, while the term $\xi^{-3}\chi_{eff}A_n^2$ is a correction-to-scaling contribution to the free energy density that describes the reduced probability of contacts between unlike (A and B) blobs.[28] From the relationship[27] $Z\xi^3 = b^3N/\phi$, the scaling result $\xi \sim \phi^{-\nu/(3\nu-1)}$, and eq 4.1 for the concentration dependence of χ_{eff}, eq 4.2 can be rewritten on a per site basis, each lattice site of volume $b^3 = 1$

$$\beta F(\phi,A_n) = \frac{\phi}{N}[2(\kappa - \phi^{\delta}wN)A_n^2 - \alpha_n A_n^3 + \beta_n A_n^4] + \upsilon_s\phi^{\mu} \tag{4.3}$$

In the above equation, $\delta = (\chi_S + 1)/(3\nu - 1) \approx 1.6$, $\mu = 3\nu/(3\nu - 1) \approx 2.3$, and υ_s is a dimensionless parameter (the counterpart of the classical excluded-volume parameter υ) that depends on the prefactor of the scaling relation $\xi \sim \phi^{-\nu/(3\nu-1)}$.

Equations 4.2 and 4.3 were obtained under the assumption that the inhomogeneous solvent concentration profiles in the weakly segregated microdomains contribute a negligible amount to the free energy. It is now convenient to reconsider this assumption. Making use of the results of ref 28, 33, and 34 discussed above, it is apparent that eq 2.38 for $p(f,\phi)$ should be modified to account for excluded-volume swelling effects by the replacements $\chi N\phi \rightarrow wN\phi^{\delta}$ and $\upsilon N\phi \rightarrow \upsilon_s N\phi^{\mu-1}$. Hence, eq 2.38 becomes

$$p(f,\phi) = H(f) + 2f(1-f)wN\phi^{\delta} + \upsilon_s N\phi^{\mu-1} \tag{4.4}$$

From eq 4.3 it is clear that $wN\phi^{\delta}$ must be the same order of magnitude as $\kappa(f)$, i.e., $O(1)$, at the semidilute MST. Since Table I shows $H(f)$ to be comparable in magnitude to $\kappa(f)$ (except for $f \rightarrow 0$ where the theory is singular), the first two terms on the right-hand side of eq 4.4 are $O(1)$ near the MST. In contrast, the third term is larger than the second by a factor of $\phi^{\mu-1-\delta} \sim \phi^{-\chi_{SD}}$. Thus, for good solvents in the semidilute-weak segregation regime $p(f,\phi) \sim \phi^{-\chi_{SD}}$, which is of order $N^{\chi_{SD}(3\nu-1)} \sim N^{0.22}$ at the overlap concentration $\phi^* \sim N^{1-3\nu}$. As a result, the term proportional to π_1^2 in eq 2.39 can be neglected if $N^{-0.22} \ll O(1)$. For sufficiently long chains we are thus justified in neglecting the contributions of solvent inhomogeneities to the free energy. Because the exponent $\chi_{SD}(3\nu - 1) \approx 0.22$ is so small, however, very long chains may be required.

Equation 4.3 can be analyzed by following the procedure used to study eq 2.40. The free energy is minimized by the choice of $A_n = \bar{A}_n$ given by eq 3.1, but with $\phi\chi$ replaced by $\phi^{\delta}w$ in eq 3.2. As before, we expand eq 4.3 about the concentration ϕ_0 that satisfies

$$\kappa - \phi_0^{\delta}wN = \alpha_n^2/8\beta_n \tag{4.5}$$

The result can be written in the form of eq 3.4 and 3.8, but with the new coefficients

$$\beta F_{00} = \upsilon_s\phi_0^{\mu} \tag{4.6}$$

$$A = 2.3\upsilon_s\phi_0^{\mu-1} - 3.1\phi_0^{\delta}wS_n^2 \tag{4.7}$$

$$B = 1.4\upsilon_s\phi_0^{\mu-2} - 4.0\phi_0^{\delta-1}wS_n^2 - 9.6\phi_0^{2\delta-1}w^2N/\beta_n \tag{4.8}$$

The coefficients A' and B' are obtained from these expressions for A and B, respectively, by setting $w = 0$. The polymer concentrations of the coexisting phases at the MST are given by eq 3.11 and 3.12 as before. In the appropriate semidilute limit, $\phi^* \ll \phi_0 \ll 1$, the width of the coexistence region turns out to be

$$(\phi_+ - \phi_-)/\phi_0 \approx 1.1\frac{w}{\upsilon_s}\phi_0^{\chi_{SD}}S_n^2 \tag{4.9}$$

Hence, due to the fact that S_n and ϕ_0 are both small in the asymptotic semidilute regime, the width of the coexistence region is again expected to be negligible. Note that as the molecular weight of the copolymers is decreased and they begin to constitute a substantial volume fraction of the solution beyond the overlap concentration, the width of the two-phase region becomes greater and, simultaneously, our ansatz regarding the neglect of solvent inhomogeneities breaks down. A more detailed analysis is required to treat this nonasymptotic semidilute regime.

As in section III, A–B composition fluctuations can be incorporated into the theory by using the Hartree approximation for the free energy. In place of eq 4.3 we use the FRH[13] expression and write for a semidilute solution of copolymer

$$\beta F(\phi,a_n) = \frac{\phi}{N}\left[\frac{1}{2\lambda}(r^2 - r_0^2) + \frac{d}{Z^{1/2}}(r^{1/2} - r_0^{1/2}) - \frac{2}{3}n\theta_n a_n^3 + \frac{1}{(2)}n\eta_n a_n^4\right] + \upsilon_s\phi^{\mu} \tag{4.10}$$

where in place of eq 3.16–3.18, we have

$$r_0 = \tau + d\lambda/(r_0Z)^{1/2} \tag{4.11}$$

$$r = \tau + d\lambda/(rZ)^{1/2} + n\lambda a_n^2 \tag{4.12}$$

$$\tau = 2[\kappa - \chi_{eff}Z]/c^2 \tag{4.13}$$

Equation 4.10 again leads one to the conclusion that the regions of two-phase coexistence are very narrow. Comparing the above expressions with those appropriate for the melt, it is apparent that the phase diagram for a semidilute solution of a diblock in a nonselective solvent can be obtained from the molten state phase diagrams generated in FRH[13] by the replacements $\chi N \rightarrow \chi_{eff}Z$ and $\bar{N} = N \rightarrow Z$. For example, the phase diagram for semidilute solutions with $Z = 10^6$ can be obtained from Figure 3 by relabeling the originate as $\chi_{eff}Z = \phi^{\delta}wN$. Chains of 10^6 blobs, however, are unphysically large. Moreover, the Hartree approximation is not quantitative at physical values of $Z \sim 10^2$. Hence, eq 4.10–4.13 should be viewed as asymptotic formulas for large Z that are merely suggestive of the qualitative features of the phase diagram at molecular weights attainable in the laboratory.

The above results lead to some interesting predictions that are best illustrated for symmetric copolymer solutions. For $f = {}^1/_2$ the MST occurs at $[\chi_{eff}Z]_t = 10.495 + 41.022Z^{-1/3}$. Using $\chi_{eff} \sim \phi^{\chi_{SD}}$ and $Z \sim N\phi^{1/(3\nu-1)}$, we find that the critical polymer volume fraction at the MST scales will molecular weight as $\phi_t \sim N^{-1/\delta} \sim N^{-0.62}$. This result is the same as that obtained in ref 29 for the demixing of A and B homopolymers in a nonselective solvent. It is also in reasonable agreement with experiments on polystyrene/polyisoprene diblock copolymers in toluene and dioctyl phthalate by Hashimoto, Shibayama, and Kawai,[18] who find $\phi_t \sim N^{-1/2}$. The authors of ref 18 stress that the experiments leading to this exponent are preliminary and that the value of –0.5 is tentative. Hence, we assign no significance to the discrepancy at this time. Our scaling result, however, is certainly in much better agreement with the experiments than the classical prediction $\phi_t \sim N^{-1}$ of ref 17–24 and section III. The present theory for semidilute solutions of diblock copolymers with good, nonselective solvents takes proper account of excluded-volume interactions and composition fluctuations, both of which were neglected in the earlier treatments.

The Hartree scattering function for the disordered phase of a semidilute diblock solution is obtained by modifying eq 3.20 in an obvious manner. We find

$$I(q) = \frac{\phi N}{\epsilon + \{F[q^2R_g^2(\phi),f] - 2\kappa\}} \quad (4.14)$$

with ϵ the solution of the equation

$$\epsilon = 2\kappa - 2\chi_{eff}Z + c^3d\lambda/(\epsilon Z)^{1/2} \quad (4.15)$$

In eq 4.14, $R_g^2(\phi)$ is the mean-squared radius of gyration of a copolymer in the semidilute regime, which is related to the correlation length and number of blobs per chain by $R_g^2(\phi) = Z\xi^2/6$. The peak in the structure factor given by eq 4.14 occurs at a wavenumber $q^* \sim R_g(\phi)^{-1} \sim \phi^{0.12}N^{-1/2}$. Experiments to test this predicted shift in the peak position with polymer volume fraction would be of interest. A second prediction that might be amenable to experimental study is for the scattering intensity at the peak wavenumber, which reaches its maximum value at the MST. For a symmetric copolymer solution, ϵ takes the value[13] $8.1114Z^{-1/3}$ at the MST, where the maximum scattering intensity is found from eq 4.14 to be

$$[I(q^*)/N\phi]_{max} = 0.12328Z^{1/3} \sim \phi^{0.44}N^{1/3} \quad (4.16)$$

V. Discussion

In the present paper we demonstrated that the addition of a nonselective, good solvent to a diblock copolymer melt leads to some new physics at the microphase separation transition (MST), namely, inhomogeneous solvent concentration profiles and the possibility of regions of two-phase coexistence. The two-phase regions, however, were shown to be so small that they are probably of no experimental consequence. Furthermore, in a good solvent the amplitudes of the solvent patterns are substantially smaller than those characterizing the A–B mesophase patterns. On the basis of these results, it was argued that to a good approximation the molten state theories of microphase separation can be extended to solutions in a straightforward manner. For concentrated copolymer solutions we obtained results that are similar to those from previous theoretical work,[17-24] but we made additional nonclassical corrections[13] to account for large-amplitude fluctuations in A–B composition near the symmetric MST. The fluctuation corrections are expected to be substantial for the molecular weights that are employed in typical block copolymer experiments. In the semidilute regime, for which there was no previous theory, we were able to modify the molten state theories to incorporate both excluded-volume and fluctuation effects. The result is a simple "blob" theory that makes a number of predictions for the scaling of the MST with polymer concentration, copolymer composition, temperature, and molecular weight. The theory also makes predictions for the full phase diagram of neutral diblock copolymer solutions, but it must be kept in mind that the present approach is restricted to the weak segregation limit and to large molecular weights.

The predictions of the theory easiest to test experimentally are likely eq 3.20 and 4.14 for the scattering function of the disordered phase and the semidilute predictions of $q^* \sim \phi^{0.12}N^{-1/2}$ for the peak position and $[I(q^*)/N\phi]_{max} \sim \phi^{0.44}N^{1/3}$ for the maximum peak intensity. A careful experimental study of the concentration dependence of the MST temperature for experiments performed at constant ϕ, or of the temperature dependence of the MST critical concentration for experiments at constant T, would also be valuable in assessing the accuracy of the theory.

Another interesting prediction of our theories for the concentrated and semidilute regimes is apparent from the phase diagrams shown in Figures 1 and 3. Namely, it should be possible by evaporating (or by some other means removing) neutral solvent to drive transitions between the various ordered phases. The figures indicate that such transitions should be easiest to observe for very high molecular weight copolymers, because the windows (in composition) that allow direct transitions between DIS and LAM and between DIS and HEX collapse to very narrow regions and the mean-field phase diagram of Figure 1 is approached in this limit. We comment that the theories for the strong segregation limit[6-9] do not predict such phase transitions between ordered structures.

Some mention should be made of the effects of polydispersity on the present results. Although we have assumed in all of our calculations that the copolymers are perfectly monodisperse, our experience with various approximate methods[43] of dealing with a narrow distribution of molecular weight leads us to expect small vertical shifts of the phase diagrams shown in Figures 1 and 3 to smaller values of the ordinate. Hence, in experimental systems there is probably a competition between fluctuation effects (included here), tending to raise $(\chi N)_t$ or $(\chi_{eff}Z)_t$, and polydispersity effects, which tend to lower these quantities. A thorough investigation of the influence of a distribution of molecular weights on the MST and microdomain structure has yet to be performed.

The results described above for the weak segregation limit of diblocks in nonselective, good solvents were obtained with relative ease because the inhomogeneities in solvent concentration turned out to be very weak. This will likely not be the case in the strong segregation limit, where a high (excess) concentration of solvent in the narrow interfacial regions could substantially lower the overall free energy. Similarly, if the neutral solvent is marginal or poor for the diblock, the inhomogeneities in solvent concentration can be comparable in amplitude to the A–B compositional inhomogeneities. Equation 2.39 is the basis for analyzing this regime in the weak segregation limit.[31]

The semidilute blob formalism developed in the present paper for copolymers and in ref 29 for the case of blends might also be extended to the *kinetics* of microphase separation or blend demixing. For example, the linear theories of spinodal decomposition by de Gennes,[37] Pincus,[38] and Binder[39] for binary homopolymer blends could be reformulated in terms of blobs to treat the early stages of demixing in systems containing a nonselective solvent component. Modifications could also be made to molten state nucleation or late stage ripening theories[40] in order to render them applicable in the presence of neutral solvent. Theories of "critical rheology" for the disordered phase of block copolymers[41] and nonequilibrium theories[42] for flow-induced structure in copolymers or blends could be similarly extended.

Acknowledgment. We are pleased to acknowledge helpful discussions with J. F. Joanny and E. Helfand.

Appendix: The RPA for Copolymer Solutions

In this Appendix we outline the extension of the classical random phase approximation (RPA)[10,27] to diblock copolymer solutions. We assume familiarity with the notation and methods of ref 10.

It is useful to explicitly write out the first-order set of RPA equations for an A–B diblock copolymer in an athermal, nonselective solvent S. To facilitate this, we define a two-component field $P_i(\mathbf{q}) = \langle \delta\phi_i(\mathbf{q}) \rangle$, where the index $i = 1$ or 2 refers to monomers of type A or B, respectively. The RPA equation set for the monomers can be written[10]

$$P_i(\mathbf{q}) = -\phi S_{ij}(q) U_j^{eff}(\mathbf{q}) \quad (A1)$$

and is to be augmented by the solvent equation

$$\langle \delta\phi_S(\mathbf{q}) \rangle = -(1-\phi)[U_S(\mathbf{q}) + U(\mathbf{q})] \quad \text{(A2)}$$

In eq A1, the effective potential (units of k_BT) acting on monomer species i is

$$U_i^{\text{eff}}(\mathbf{q}) = U_i(\mathbf{q}) + U(\mathbf{q}) + V_{ij}P_j(\mathbf{q}) \quad \text{(A3)}$$

with $V_{11} = V_{22} = 0$ and $V_{12} = V_{21} = \chi$. The first contribution on the rhs of eq A3, $U_i(\mathbf{q})$, is an external potential that can force a direct response (i.e., a change in concentration) of species i. The second term, $U(\mathbf{q})$, is a self-consistent potential that acts uniformly on all three species (A, B, and S) and ensures incompressibility. Finally, $V_{ij}P_j(\mathbf{q})$ describes the chemical potential arising from interactions between A and B monomers. Because the solvent is assumed to be athermal, $U_i^{\text{eff}}(\mathbf{q})$ contains no terms arising from copolymer–solvent interactions. It is important to note that the effective potential that enters the solvent equation (A2) has only the first two types of contributions.

In eq A1, $\mathbf{S}(q)$ is the 2×2 matrix of ideal correlation functions for a *melt* of noninteracting Gaussian diblock chains. The elements of this matrix are given in eq 2.10–2.12. The explicit factors of polymer volume fraction ϕ in eq A1 and solvent volume fraction $1 - \phi$ in eq A2 weight the ideal response functions by the appropriate amount of polymer or solvent present in the solution.

The self-consistent potential is chosen in the RPA to ensure that incompressibility of the three species system is satisfied, i.e., $\langle \delta\phi_S(\mathbf{q}) \rangle = -P_1(\mathbf{q}) - P_2(\mathbf{q})$. Thus, we can eliminate $\langle \delta\phi_S(\mathbf{q}) \rangle$ from eq A2 to find for $U(\mathbf{q})$

$$U(\mathbf{q}) = v[P_1(\mathbf{q}) + P_2(\mathbf{q})] - U_S(\mathbf{q}) \quad \text{(A4)}$$

where $v = 1/(1-\phi)$ is the excluded-volume parameter. Substitution of this result into eq A3 gives for the effective potential

$$U_i^{\text{eff}}(\mathbf{q}) = U_i(\mathbf{q}) + W_{ij}P_j(\mathbf{q}) \quad \text{(A5)}$$

with $W_{11} = W_{22} = v$ and $W_{12} = W_{21} = \chi + v$ and where we have dropped the external solvent potential. Equations A1 and A5 are now a closed set of linear equations for the two-element vector $P_i(\mathbf{q})$. The solution can be written

$$P_i(\mathbf{q}) = -\tilde{S}_{ij}(q)U_j(\mathbf{q}) \quad \text{(A6)}$$

where in matrix notation

$$\tilde{\mathbf{S}}(q) = [\phi^{-1}\mathbf{S}^{-1}(q) + \mathbf{W}]^{-1} \quad \text{(A7)}$$

Equation A7 is the classical RPA expression for the scattering function matrix $\tilde{S}_{ij}(q) = V^{-1}\langle \delta\phi_i(\mathbf{q})\delta\phi_j(-\mathbf{q}) \rangle$. As we shall see below, the inverse of $\tilde{\mathbf{S}}(q)$ determines the quadratic term in the free energy expression 2.3.

Having eliminated $\langle \delta\phi_S(\mathbf{q}) \rangle$ by the incompressibility condition, the above set of first-order RPA equations for a copolymer solution involve only the two monomer fields $P_1(\mathbf{q})$ and $P_2(\mathbf{q})$. In fact, these equations are identical with those of Leibler[10] for a diblock melt, except that the interaction matrix $\mathbf{W}$ is of a different form and there is (here) an explicit factor of ϕ attached to the $S_{ij}(q)$. It turns out that this similarity in the structure of the equations holds to all orders in the RPA. Thus, the higher order equations for a copolymer solution can be obtained directly from the melt expressions of ref 10. We state here the results of solving these equations to fourth order in $U_i(\mathbf{q})$ [and, thus, to fourth order in $P_i(\mathbf{q})$.] The Legendre-transformed free energy [as a functional of $P_i(\mathbf{q})$] can be written

$$\beta F = \beta F + \frac{1}{2!}V^{-2}\sum_{\mathbf{q}_1\mathbf{q}_2}\Phi_{ij}^{(2)}(\mathbf{q}_1,\mathbf{q}_2)P_i(\mathbf{q}_1)P_j(\mathbf{q}_2) + \frac{1}{3!}V^{-3}\sum_{\mathbf{q}_1\mathbf{q}_2\mathbf{q}_3}\Phi_{ijk}^{(3)}(\mathbf{q}_1,\mathbf{q}_2,\mathbf{q}_3)P_i(\mathbf{q}_1)P_j(\mathbf{q}_2)P_k(\mathbf{q}_3) + \frac{1}{4!}V^{-4}\sum_{\mathbf{q}_1\cdots\mathbf{q}_4}\Phi_{ijkl}^{(4)}(\mathbf{q}_1,\mathbf{q}_2,\mathbf{q}_3,\mathbf{q}_4)P_i(\mathbf{q}_1)P_j(\mathbf{q}_2)P_k(\mathbf{q}_3)P_l(\mathbf{q}_4) \quad \text{(A8)}$$

where

$$\Phi_{ij}^{(2)}(\mathbf{q}_1,\mathbf{q}_2) = \delta^K(\mathbf{q}_1+\mathbf{q}_2)[\phi^{-1}S_{ij}^{-1}(\mathbf{q}_1) + W_{ij}] \quad \text{(A9)}$$

$$\Phi_{ijk}^{(3)}(\mathbf{q}_1,\mathbf{q}_2,\mathbf{q}_3) = -\phi G_{lmn}^{(3)}(\mathbf{q}_1,\mathbf{q}_2,\mathbf{q}_3)[\phi^{-1}S_{il}^{-1}(\mathbf{q}_1)] \times [\phi^{-1}S_{jm}^{-1}(\mathbf{q}_2)][\phi^{-1}S_{kn}^{-1}(\mathbf{q}_3)] \quad \text{(A10)}$$

$$\Phi_{ijkl}^{(4)}(\mathbf{q}_1,\mathbf{q}_2,\mathbf{q}_3,\mathbf{q}_4) = \phi\{V^{-1}\sum_{\mathbf{q}_5}S_{oq}^{-1}(\mathbf{q}_5) \times [G_{mno}^{(3)}(\mathbf{q}_1,\mathbf{q}_2,\mathbf{q}_5)G_{qpr}^{(3)}(-\mathbf{q}_5,\mathbf{q}_3,\mathbf{q}_4) + G_{mpo}^{(3)}(\mathbf{q}_1,\mathbf{q}_3,\mathbf{q}_5)G_{qnr}^{(3)}(-\mathbf{q}_5,\mathbf{q}_2,\mathbf{q}_4) + G_{mro}^{(3)}(\mathbf{q}_1,\mathbf{q}_4,\mathbf{q}_5)G_{qpn}^{(3)}(-\mathbf{q}_5,\mathbf{q}_3,\mathbf{q}_2)] - G_{mnpr}^{(4)}(\mathbf{q}_1,\mathbf{q}_2,\mathbf{q}_3,\mathbf{q}_4)\}[\phi^{-1}S_{im}^{-1}(\mathbf{q}_1)][\phi^{-1}S_{jn}^{-1}(\mathbf{q}_2)] \times [\phi^{-1}S_{kp}^{-1}(\mathbf{q}_3)][\phi^{-1}S_{lr}^{-1}(\mathbf{q}_4)] \quad \text{(A11)}$$

The Gaussian correlation functions $G_{ijk}^{(3)}$ and $G_{ijkl}^{(4)}$ appearing in the above equations are those for a melt of diblock molecules (i.e., the only dependence on ϕ is explicit) and are given in Appendices B and C of ref 10.

To obtain the desired eq 2.3, we insert into eq A8 the change of variables $P_i(\mathbf{q}) = M_{ij}^{-1}\psi_j(\mathbf{q})$, where $\mathbf{M}$ is defined in eq 2.2. A free energy expression of the form of eq 2.3 results, with $\mathbf{R}(q)$ in eq 2.6 given by

$$\mathbf{R}(q) = (\mathbf{M}^{-1})^{\mathrm{T}}[\phi^{-1}\mathbf{S}^{-1}(q) + \mathbf{W}]\mathbf{M}^{-1} \quad \text{(A12)}$$

and with $\mathbf{Q}(q)$ in eq 2.15 and 2.16 given by

$$\mathbf{Q}(q) = \phi^{-1}(\mathbf{M}^{-1})^{\mathrm{T}}\mathbf{S}^{-1}(q) \quad \text{(A13)}$$

The superscript T in eq A12 and A13 represents the matrix transpose. Explicit evaluation of the rhs of eq A12 leads to eq 2.7–2.9 and the rhs of eq A13 gives rise to eq 2.17–2.20. QED.

References and Notes

(1) *Block Copolymers*; Aggarwal, S. L., Ed.; Plenum Press: New York, 1970.
(2) *Developments in Block Copolymers-I*; Goodman, I., Ed.; Applied Science Publishers: New York 1982.
(3) Thomas, E. L.; Alward, D. B.; Kinning, D. J.; Martin, D. C.; Handlin, D. L.; Fetters, L. J. *Macromolecules* **1986**, *19*, 2197.
(4) Leary, D. F.; Williams, M. C. *J. Polym. Sci., B* **1970**, *8*, 335.
(5) Meier, D. J. *J. Polym. Sci., C* **1969**, *26*, 81.
(6) Helfand, E. *Macromolecules* **1975**, *8*, 552.
(7) Helfand, E.; Wasserman, Z. *Polym. Eng. Sci.* **1977**, *17*, 582.
(8) Semenov, A. N. *Sov. Phys. JETP* **1985**, *61*, 733.
(9) Ohta, T.; Kawasaki, K. *Macromolecules* **1986**, *19*, 2621.
(10) Leibler, L. *Macromolecules* **1980**, *13*, 1602.
(11) Bates, F. S.; Hartney, M. A. *Macromolecules* **1985**, *18*, 2478.
(12) Mori, K.; Hasegawa, H.; Hashimoto, T. *Polym. J. Jpn.* **1985**, *17*, 799.
(13) Fredrickson, G. H.; Helfand, E. *J. Chem. Phys.* **1987**, *87*, 697.
(14) Brazovskii, S. A. *Sov. Phys. JETP* **1975**, *41*, 85.
(15) Amit, D. J. *Field Theory, the Renormalization Group, and Critical Phenomena*; World Scientific: New York, 1984.
(16) Bates, F. S. *Macromolecules* **1984**, *17*, 2607.
(17) Shibayama, M.; Hashimoto, T.; Hasegawa, H.; Kawai, H. *Macromolecules* **1983**, *16*, 1427.
(18) Hashimoto, T.; Shibayama, M.; Kawai, H. *Macromolecules* **1983**, *16*, 1093.
(19) Shibayama, M.; Hashimoto, T.; Kawai, H. *Macromolecules* **1983**, *16*, 1434.
(20) Pico, E. R.; Williams, M. C. *Polym. Eng. Sci.* **1977**, *17*, 573.
(21) Pico, E. R.; Williams, M. C. *J. Appl. Polym. Sci.* **1978**, *22*, 445.
(22) Hugenberger, G. S.; Williams, M. C. *Macromolecules*, in press.
(23) Noolandi, J.; Hong, K. M. *Ferroelectrics* **1980**, *30*, 117.
(24) Hong, K. M.; Noolandi, J. *Macromolecules* **1983**, *16*, 1083.

(25) Bates, F. S.; Wignall, G. D. *Phys. Rev. Lett.* **1986**, *57*, 1429.
(26) Landau, L. D.; Lifshitz, E. M. *Statistical Physics-Part 1*, 3rd ed.; Pergamon Press: New York, 1980.
(27) de Gennes, P.-G. *Scaling Concepts in Polymer Physics*; Cornell University Press: Ithaca, NY, 1979.
(28) Joanny, J. F.; Leibler, L.; Ball, R. *J. Chem. Phys.* **1984**, *81*, 4640.
(29) Broseta, D.; Leibler, L.; Joanny, J. F. *Macromolecules* **1987**, *20*, 1935.
(30) Note that we have only shown q^* to be the most unstable wavenumber for the symmetric case of $f = {}^1/_2$. Justification of this wavenumber for patterns formed by asymmetric systems follows a posteriori by the demonstration that patterns with wavenumbers $q_0 \neq q^*$ have a larger free energy than those characterized by q^*.
(31) Leibler, L.; Fredrickson, G. H. Manuscript in preparation.
(32) In the calculations of ref 13 for diblock melts it was assumed (in the spirit of a lattice theory) that $\rho_m = b^{-3}$. This condition, however, is usually not satisfied in experimental systems. Relaxation of the condition leads to the replacement of N by $\bar{N} = Nb^6\rho_m^2$ in the fluctuation corrections computed by FRH. It is important to note that $\bar{N}$ does not depend on the definition of a statistical segment, as it can be expressed in terms of observables by $\bar{N} = (6R_g^2\rho_c^{2/3})^3$. An incorrect expression for $\bar{N}$, different from the ones above, was given in ref 13.
(33) Schafer, L.; Kappeler, Ch. *J. Phys. (Les Ulis, Fr.)* **1985**, *46*, 1853.
(34) Kosmas, M. K. *J. Phys. Lett.* **1984**, *45*, L-889.
(35) Broseta, D.; Leibler, L.; Kaddour, L. O.; Strazielle, C. *J. Chem. Phys.* **1987**, *87*, 7248.
(36) F. Bates, private communication.
(37) de Gennes, P.-G. *J. Chem. Phys.* **1980**, *72*, 4756.
(38) Pincus, P. *J. Chem. Phys.* **1981**, *75*, 1996.
(39) Binder, K. *J. Chem. Phys.* **1983**, *79*, 6387.
(40) Onuki, A. *J. Chem. Phys.* **1986**, *85*, 1122.
(41) (a) Fredrickson, G. H.; Larson, R. G. *J. Chem. Phys.* **1987**, *86*, 1553. (b) Onuki, A. *J. Chem. Phys.* **1987**, *87*, 3692. (c) Fredrickson, G. H.; Helfand, E. *J. Chem. Phys.* **1988**, *89*, 5890.
(42) Fredrickson, G. H. *J. Chem. Phys.* **1986**, *85*, 5306.
(43) Leibler, L.; Benoit, H. *Polymer* **1981**, *22*, 195.

Influence of Star-Core Exclusion on Polymer–Polymer Miscibility

Anne B. Faust,† Paul S. Sremcich, and John W. Gilmer*,‡

Penn State University, University Park, Pennsylvania 16802

Jimmy W. Mays*

Department of Chemistry, University of Alabama at Birmingham, Birmingham, Alabama 35294. *Received April 21, 1988; Revised Manuscript Received July 27, 1988*

ABSTRACT: In this study the effect was investigated of the high functionality branch point in the star-shaped polystyrene (PS) molecule on the shape of its phase diagram when mixed with poly(vinyl methyl ether) (PVME). A comparison was made between samples containing a 22-arm star-shaped PS blended with linear PVME and the linear/linear blend comprised of components of the same molecular weight. These materials were characterized by wide-angle light-scattering cloud-point analyses utilizing both ramp and stepwise heating to properly separate thermodynamic and kinetic effects. Although the temperature minima for the cloud-point curves of both the star/linear blend and the linear/linear blend are the same, the curve for the star/linear system is shifted to the polystyrene-rich side of the composition axis. From this shift, a value of 0.27 is determined as the fraction of the star sterically hindered from interacting with neighboring molecules.

Introduction

Recently it has been increasingly noted that the phase behavior of multicomponent polymers can be changed not only by varying their intercomponent interaction and their molecular weights but also by modifying the molecular design of the molecules. Factors such as copolymer block length, degree of branching or cross-linking, chain stiffness, and overall copolymer architecture affect the morphology and phase behavior of a material.

A star molecule is a good model system to study exclusion due to multiple functionality branching in polymers. The role of steric hindrance resulting from a multiple junction may be studied by analyzing the phase diagram of a blend containing star-shaped molecules. By substitution of a star polymer in place of a linear one of the same type and molecular weight, the changes which result in the phase diagram can be utilized to obtain information concerning the exclusion exhibited in the core region.

In this study, the phase behavior of the poly(vinyl methyl ether) (PVME)/polystyrene (PS) blend system was characterized. Wide-angle light-scattering cloud-point analysis was used to determine the miscibility limit of this blend system. Binary mixtures of polystyrene and poly(vinyl methyl ether) were among the first blends to be studied and were investigated by a number of techniques, including optical and electron microscopy, differential scanning calorimetry (DSC), light and neutron scattering, NMR and IR spectroscopy, and excimer fluorescence.[1-9] Special attention has been devoted to this blend because it possesses an experimentally accessible LCST, below which it exhibits complete miscibility. Thus it serves as an excellent system in which to study the phase-separation behavior of polymers.

The cloud-point curve allows the practical determination of the binodal and can be detected by optical microscopy or by wide-angle light scattering. The cloud-point curve is established by measuring the temperatures at which clear (miscible) blends become turbid. This method can be used when the refractive indices of the two components are significantly different with the assumption that phase separation in the blend is sufficiently rapid to allow an accurate determination of the demixing temperature.

According to the thermodynamics of mixtures, the most influential factors which determine whether or not an LCST is exhibited in a polymer–polymer mixture are the interaction between components and the thermal expansion parameters.[10] The precise position of the phase-sep-

† Present address: RayChem Corporation, Fuquay-Varina, NC 27526.
‡ Present address: EniChem Americas Inc., Monmouth Junction, NJ 08852.

0024-9297/89/2222-1250$01.50/0